Lawrence Berkeley National Laboratory
Recent Work

Title
Higher climatological temperature sensitivity of soil carbon in cold than warm climates

Permalink
https://escholarship.org/uc/item/7q68v57x

Journal
Nature Climate Change, 7(11)

ISSN
1758-678X

Authors
Koven, CD
Hugelius, G
Lawrence, DM
et al.

Publication Date
2017-11-01

DOI
10.1038/nclimate3421

Peer reviewed

Higher Climatological Temperature Sensitivity of Soil Carbon in Cold Than Warm Climates

C. D. Koven[1*], G. Hugelius[2,3], D. M. Lawrence[4], W. R. Wieder[4,5]

5

Affiliations:

[1]Earth and Environmental Sciences Division, Lawrence Berkeley National Laboratory, Berkeley, CA, USA

10

[2]Department of Physical Geography & Bolin Centre of Climate Research, Stockholm University, Stockholm, Sweden

[3] School of Earth, Energy, and Environmental Sciences, Stanford University, Stanford, CA, USA

15

[4]Climate & Global Dynamics Laboratory, National Center for Atmospheric Research, Boulder, CO, USA

[5]Institute of Arctic & Alpine Research, University of Colorado, Boulder, CO, USA

20

*Correspondence to: cdkoven@lbl.gov

25 The projected loss of soil carbon to the atmosphere resulting from climate change is a potentially large but highly uncertain feedback to warming. The magnitude of this feedback is poorly constrained by observations and theory, and is disparately represented in Earth system models (ESMs)[1-3]. To assess the climatological temperature sensitivity of soil carbon, we calculate apparent soil carbon turnover times[4] that reflect long-term and broad-scale rates of

30 decomposition. Here, we show that the climatological temperature control on carbon turnover in the top meter of global soils is more sensitive in cold climates than in warm ones and argue that it is critical to capture this emergent ecosystem property in global-scale models. We present a simplified model that explains the observed high cold-climate sensitivity using only the physical scaling of soil freeze-thaw state across climate gradients. Current ESMs fail to capture this

35 pattern, except in an ESM that explicitly resolves vertical gradients in soil climate and C turnover. An observed weak tropical temperature sensitivity emerges in a different model that explicitly resolves mineralogical control on decomposition. These results support projections of strong carbon-climate feedbacks from northern soils[5,6] and demonstrate a method for ESMs to capture this emergent behavior.

40

Carbon cycle feedbacks represent a large uncertainty on the terrestrial response to climate change[1-3]. Much of this uncertainty arises from the dynamics of decomposing soil carbon under changing climate, in particular how the rate of carbon cycling through soils may change with warming. Fast-timescale observations[7] and general kinetic theory[8] both suggest that

45 decomposition rates should increase with warming. While this temperature response has long been thought to provide a positive feedback to warming[9], its magnitude is poorly quantified due to the many confounding factors affecting soil metabolic rates[8]. Furthermore, acclimatory responses by soil microbiota that reduce the effect of warming on decomposition rates at longer timescales have been proposed[10-12] to explain the reduction in temperature sensitivity observed in

50 experiments[13]. Given the size of global soil C stocks, especially at high latitudes[14] and the potential long-term vulnerability of soil C to warming, it is critical to accurately include these feedbacks in assessing emissions scenarios that are compatible with desired climate outcomes[15].

The current (Coupled-Model Intercomparison Project, phase 5; CMIP5) generation of ESMs actually show a relatively small contribution of climate-driven changes to carbon turnover times

on soil carbon stocks, with the majority of projected soil carbon change instead occurring due to changes in plant productivity[3]. The ESMs—which couple carbon cycle and climate processes—typically use simplified temperature sensitivities[12], omit realistic dynamics of soil microbial ecology[16], show little predictive power in simulating current soil carbon stocks[17], and systematically overestimate the transient sensitivity of soil carbon pools to productivity changes[18]. Equally troubling, the models omit crucial processes that may exacerbate warming-related carbon losses, in particular the representation of frozen carbon in permafrost soils[6]. Thus, although ESMs show high inter-model divergence in soil carbon predictions, they likely underestimate the actual uncertainty[16] surrounding increased atmospheric greenhouse gas burdens and accelerated warming under climate change scenarios.

It is difficult to directly evaluate the transient climate-response predictions made by ESM soil carbon models, because dynamical observations of soil carbon responses to warming at the relevant timescale—multi-decadal to centennial—are scarce[16] and ambiguous about both acclimation timescales and whether changes result from productivity or turnover responses[19]. An alternate approach is to look at model predictions across spatial gradients, since current soil conditions reflect the long-term accumulated effects of climate, vegetation, edaphic properties, and landscape changes on soil organic matter formation[20] (see Methods). Indeed, the large spatial variation of soil carbon turnover times across climate gradients served as an early piece of evidence supporting the idea that warming would lead to soil carbon losses[21,22].

Because the balance of carbon inputs and decomposition determine soil carbon stocks, and because both of these controls are mediated by climate, it is useful to separate them by defining an apparent turnover time, τ, as the ratio of carbon losses via heterotrophic respiration to total carbon stocks. Since, at steady state, carbon losses and inputs are equal, and because we have more robust global estimates of productivity than of heterotrophic respiration, we assume that soils are approximately at steady state in order to estimate τ as the ratio of carbon stocks to carbon inputs[4].

In figure 1 we show the global distribution of soil carbon stocks (fig. 1a), vegetation inputs to soil (fig. 1b), and τ, as a function of temperature and precipitation (fig. 1c). These results illustrate that τ is clearly sensitive to both soil temperature and moisture, but here we are primarily interested in identifying the temperature control on soil carbon turnover. Moisture may

dominate turnover in places that are either highly moisture-limited[4] or saturated, so we mask all points where we expect moisture to exert a dominant control (fig. S1), to isolate the temperature-dominated soil carbon τ response (fig. 1d). This relationship clearly shows a change in the sensitivity of inferred τ to climatological temperature over the interval, with stronger sensitivity in cold climates than in warm ones. We note, however, that considerable variation remains. The residual two-fold variation in turnover times (residual variance in $\log(\tau) = 0.1$; table S1) is also a real and important feature of the data, and this may be driven by mineralogical or other factors[23,24] beyond the simple climate metrics used here. We recognize that further research diagnosing the mechanisms responsible for this variation is critical, but here we focus on the central relationship between soil τ and temperature that emerges from our global analysis.

Taking the derivative of the central soil τ to temperature relationship (fig. 1d), and placing this in terms of the exponential form Q_{10}, gives a "climatological Q_{10}" (fig. 2), which decreases with temperature, from $Q_{10}>5$ in cold climates to $Q_{10}=1$ (i.e. no temperature sensitivity) in hot climates. This climatological Q_{10} differs from the classical short-timescale Q_{10} in being diagnosed from the τ, whereas short-timescale Q_{10} values are diagnosed based on instantaneous decay rates, k (where, at steady state, $k = 1/\tau$). Short-timescale respiration observations show a widespread Q_{10}-like behavior with a value in the range of approximately 1.4 based on eddy covariance fluxes[7], or 1.5-2 based on soil incubations[8]. Where the climatological Q_{10} value differs from the short- timescale Q_{10} value, this is evidence for emergent behavior at longer timescales that leads to the divergence between short- and long- timescale temperature sensitivities. We thus divide the world heuristically into three roughly defined regimes (fig. 2): a cold-climate high-sensitivity emergent domain (climatological $Q_{10}\sim2$ to 5), a temperate non-emergent domain (climatological $Q_{10}\sim1.4$ to 2), and possibly a warm-climate low-sensitivity emergent domain (climatological $Q_{10}<1.4$).

To understand why the climatological Q_{10} exceeds short-timescale Q_{10} values in cold climates, we explore a hierarchy of simplified decomposition models. These derive τ values based solely on modeled soil temperature (T) dynamics and differ only in the functional form of k(T) and how this is scaled in space and time to calculate τ (fig. 3). We consider four cases. The first three differ only in the form of k(T) and all use near-surface soil temperatures (10 cm): fixed Q_{10} over the entire temperature range, (fig. 3a); temperature-sensitive Arrhenius relationship[25] over the entire temperature range, (fig. 3b); fixed Q_{10} over thawed temperatures and no

respiration when soil is frozen (fig. 3c). The fourth case shown uses the same temperature function as the third, but diagnoses k using depth-resolved soil temperatures over the full 0-1m depth interval (fig. 3d). Only the fourth case is able to qualitatively capture the observed change in slope seen in the observations.

120   The implication of the curve in figure 3d is that the increase in temperature sensitivity in cold climates can be explained simply as a result of the combined reductions in the thawed season length and thawed depth during the warm season. Thus, vertical variation in soil climate must be accounted for to explain carbon stocks at high latitudes, even when considering carbon to only 1m depth. Models that explicitly resolve this process, by replacing traditional carbon

125   cycle ordinary differential equations (ODEs) with a set of vertically resolved partial differential equations (PDEs) that include transport, are one such approach, but suffer from high uncertainty in the rates of cold-soil vertical mixing processes, such as cryoturbation[6]. Those long-term mixing processes also contribute significantly to the large amounts of carbon stored even deeper, below 1 meter depth[14,26], which add further uncertainty and bias to global carbon cycle

130   projections. That a simpler ODE approach using a depth-averaged k approximates the observed relationship suggests that, at least in the near surface, such transport processes are sufficiently fast over long timescales for the soil to act as a well-mixed reservoir through which respiration can occur at any depth within the 0-1m interval.

        We contend that the climatological sensitivity of soil C to historical climate (fig. 1d) is an

135   emergent ecosystem property that models should be expected to replicate. To test whether ESMs are able to match these qualitative patterns, we compare predictions of τ from models used in the CMIP5 carbon cycle experiments (fig. 4a-f, table S2)[1]. Most models show a linear relationship between $\log(\tau)$ and MAAT, as would result from using fixed Q_{10} and a single-layer model that diagnoses k values from near-surface temperatures. Some models show offsets and emergent

140   behavior, but none are able to qualitatively capture both the increase in temperature sensitivity through the entire range of cold climates as well as the reduction in temperature sensitivity in tropical climates shown by the global data. The inability of the models to match spatial gradients implies that the transient response to warming will likewise be biased, particularly in the cold-climate regime where the ESMs show a systematic underestimate of the climate sensitivity on

145   soil carbon turnover. That the ESMs also show weak turnover-driven soil carbon responses to

warming[3], and a net high-latitude carbon gain from warming[2], is thus likely a shared artifact of the weak temperature control in these ESMs.

Because none of the CMIP5 models represent permafrost carbon dynamics, we diagnose the same relationship from a model which does represent permafrost carbon via a PDE approach, CLM4.5[27] (fig. 4g-h). The two panels 4g and 4h differ only by a parameter, Z_τ, that controls decomposition rates k at depth, beyond the resolved climatologic controls. The parameter is defined as an e-folding depth, and a short value assumes that the base decomposition rate (k) of deeper soil horizons is intrinsically slower than surface soil carbon stocks (Fig. 4g). A long e-folding depth assumes that carbon pools in surface and deep soil horizons have similar intrinsic decomposability, which allows climatologic controls (e.g., temperature) to more strongly influence decomposition rates (Fig. 4h). The model is able to match the observed increase in sensitivity at cold climates, but only when the base rates of deep decomposition are more similar to those at the surface (fig. 4h). Under these conditions CLM4.5 predicts a substantial (-23 Pg C/˚C) destabilizing carbon-climate feedback from the permafrost region[28], which contrasts in sign with the stabilizing feedback projected by the CMIP5 ESMs from this region. The patterns of τ in fig. 4h better match observations in fig. 1 than other models analyzed here (Table S1), suggesting that the corresponding projection of a strong permafrost carbon-climate feedback is also more realistic.

The wide spread in τ (Fig 1d) and the low-sensitivity emergent domain observed in warm climates (Fig. 2) emerges from a model that includes mineral and microbial associations (fig. 4i). This mineral/microbial model predicts longer τ values for the clay rich tropical soils and therefore a reduced sensitivity to temperature. Because weathering rates increase with temperature in sufficiently moist ecosystems, clay amounts and temperature are positively correlated, which may explain the reduced tropical temperature sensitivity (fig. S3). However, the reduced sensitivity of tropical soil carbon is also consistent with nonlinear models that predict a temperature optimum for decomposition[29], though only at tropical temperatures. Separating these potential causes is not possible with the static benchmark proposed here, but is of great importance, as they would lead to different trajectories under global warming.

We propose that global temperature control on turnover, as expressed in spatial gradients, is a useful benchmark on dynamic models, which must predict these static relationships if we are

to have confidence in their transient responses. We recognize that projections of soil C response to warming are complicated by changes in plant productivity, organo-mineral stabilization, soil-aggregate formation and shifts in belowground community structure and function[30]. Indeed, resolving these complex interactions should be a focus for the next generation of experiments and models[16]. The results shown here stress the importance of considering temperature effects on decomposition across the full range of climates found on Earth, as well as vertically, even within the top meter of soils. The systematic underestimation by the CMIP5 models of the sensitivity of carbon turnover in cold climates belies their projections of weak soil turnover-driven feedbacks to warming. Thus the relationships shown here support stronger carbon – climate feedbacks— particularly from northern regions—than current estimates suggest.

Figures
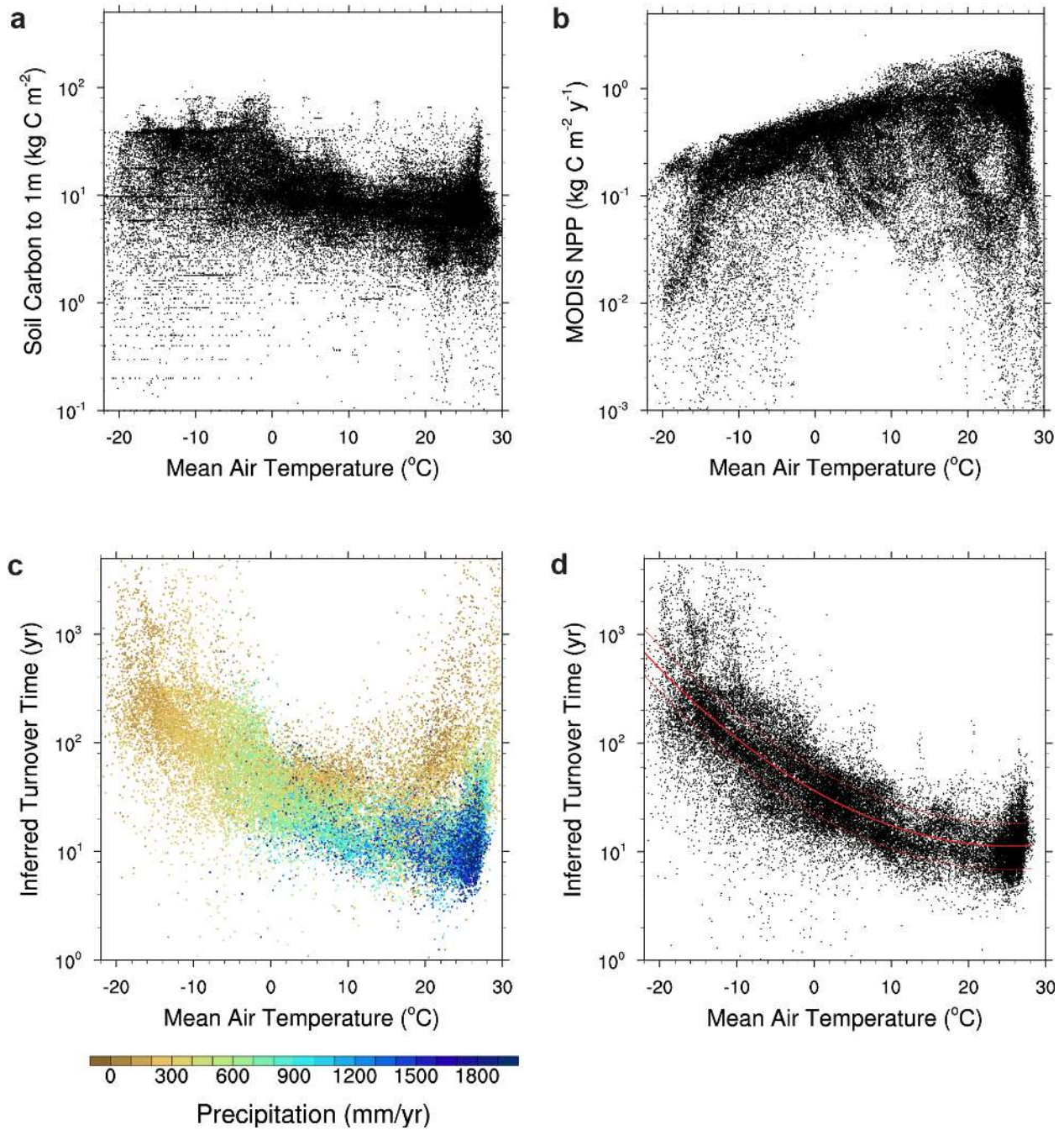
Fig. 1. **Global distributions of the inferred apparent turnover time (τ) of global soil organic matter as function of climatological temperature**. τ is calculated as the ratio of (a) carbon stocks to (b) net primary productivity. (c) τ plotted as function of Mean Annual Air Temperature (MAAT). Each gridcell is colored by climatological precipitation. (d) As in (c), but after filtering out gridcells that are likely to be dominated by either aridity (P minus PET < threshold of -1000

mm/yr) or saturation (peatland fraction exceeds threshold of 50%). Best fit regression curve in (d) uses a quadratic regression of $\log(\tau)$ versus MAAT, with 50% prediction intervals shown.

200
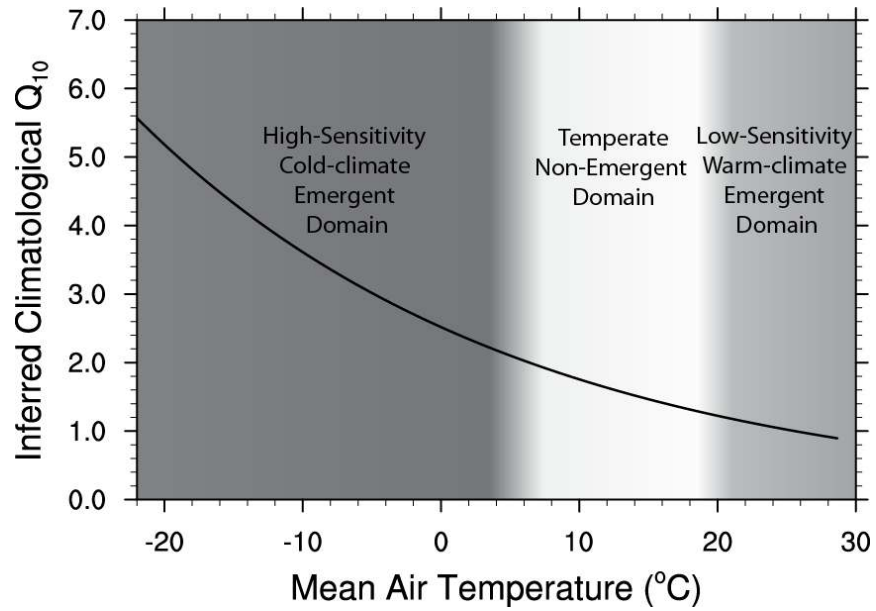
Fig 2. Inferred "climatological Q_{10}" as a function of temperature. Climatological Q_{10} is calculated from the derivative of the regression relationship between τ and MAAT in fig. 1d. We define emergent domains as those where the climatological Q_{10} differs appreciably from short-term Q_{10} values (i.e $Q_{10} > 2$ or $Q_{10} < 1.4$).
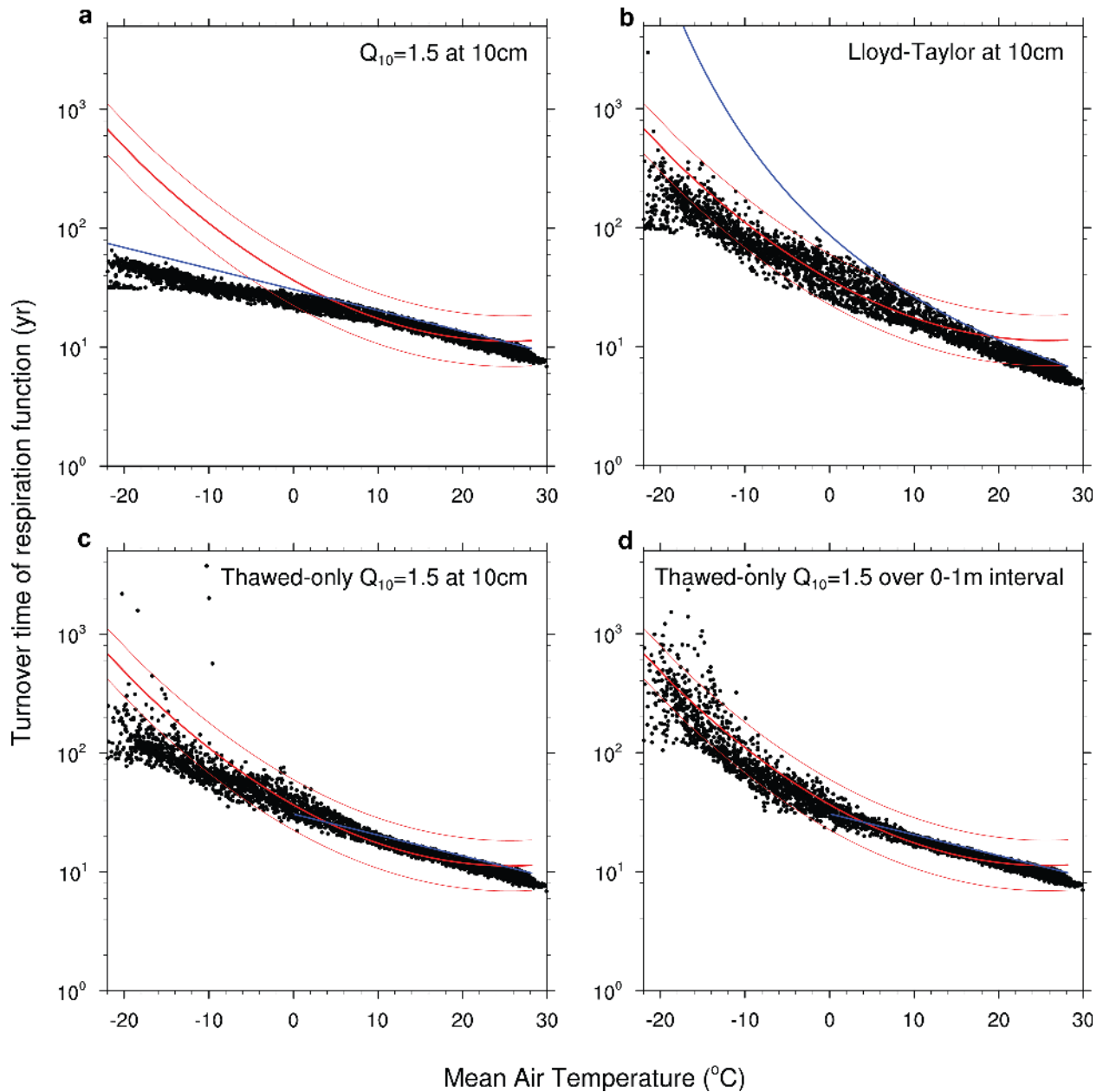
Fig. 3 A hierarchy of simplified models to explain the cold-climate emergent regime of high climatological temperature sensitivities. In all cases, τ is calculated using daily soil temperatures from a land surface model, applying a simplified decomposition function to derive daily decomposition rates (k), and inferring τ as the reciprocal of the mean decomposition function k. (a) Simple $Q_{10}=1.5$ function evaluated. (b) Arrhenius temperature function. (c) Thawed-only $Q_{10}=1.5$ function evaluated at 10cm depth. (c) Thawed-only $Q_{10}=1.5$ function

averaged over the surface-1m depth interval. Blue lines are the decomposition function as evaluated on MAAT. Red lines are the best-fit curve and prediction intervals are from fig. 1d.
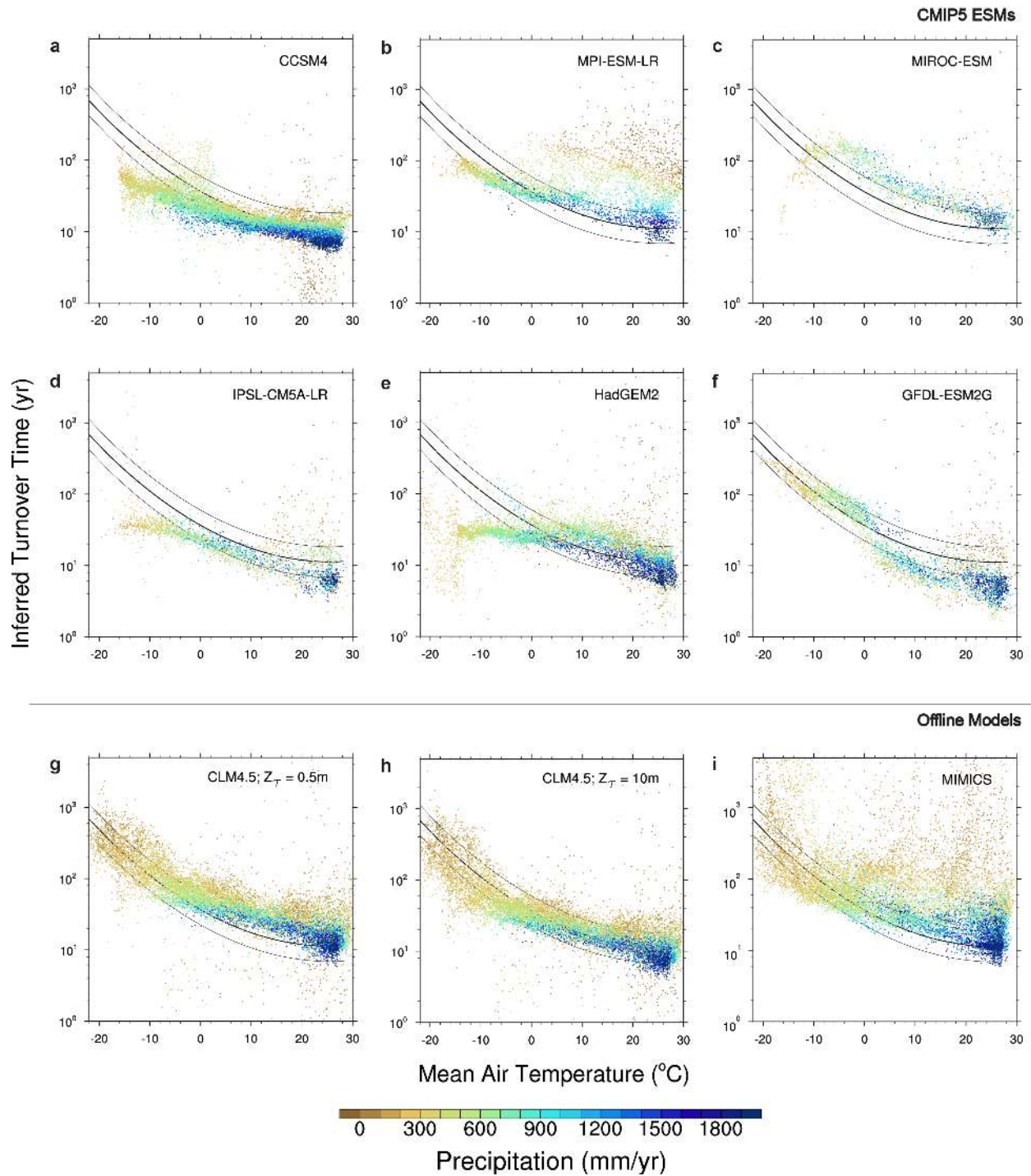
220

Fig. 4 A comparison of relationships between soil turnover times and climate as predicted by a suite of ESMs and offline land models. Inferred apparent turnover time, τ, calculated as in figure 1 and colored by precipitation as in fig 1c, from soil models used in Earth system models. (a-f) CMIP5 models, each of which (other than GFDL-ESM2G) use single-layer soil temperature

225 control on soil carbon turnover. (g-h) CLM4.5, which calculates vertically-resolved

13

decomposition rates. (g) and (h) differ by varying a parameter (Z_τ) that controls decomposition rates with depth independently from resolved temperature, moisture, and oxygen controls (i) MIMICS, which treats decomposition as a microbially-enabled and mineral-resolved nonlinear model, shows the wide scatter in moist tropical climates as observed, due to its consideration of mineralogical control on decomposition.

Author Contributions

CDK designed the study and performed analyses, based on ideas developed through discussions

255 with DML, GH, and WRW. WRW contributed MIMICS results, CDK and DML contributed

CLM4.5 results, and GH contributed NCSCD data. All authors wrote the manuscript.

References (Main Text)

260

1 Arora, V. K. *et al.* Carbon-concentration and carbon-climate feedbacks in CMIP5 Earth system models. *Journal of Climate* **26**, 5289-5314, doi:10.1175/JCLI-D-12-00494.1 (2013).

2 Ciais, P. *et al.* in *Climate Change 2013: The Physical Science Basis. Contribution of Working Group I to the Fifth Assessment Report of the Intergovernmental Panel on Climate Change* (eds T.F. Stocker *et al.*) (Cambridge University Press, 2013).

265

3 Koven, C. D. *et al.* Controls on terrestrial carbon feedbacks by productivity versus turnover in the CMIP5 Earth System Models. *Biogeosciences* **12**, 5211--5228, doi:10.5194/bg-12-5211-2015 (2015).

4 Carvalhais, N. *et al.* Global covariation of carbon turnover times with climate in terrestrial ecosystems. *Nature* **514**, 213-217, doi:10.1038/nature13731 (2014).

270

5 Ciais, P. *et al.* Large inert carbon pool in the terrestrial biosphere during the Last Glacial Maximum. *Nature Geosci* **5**, 74-79, doi:10.1038/ngeo1324 (2012).

6 Koven, C. D. *et al.* Permafrost carbon-climate feedbacks accelerate global warming. *Proceedings of the National Academy of Sciences* **108**, 14769--14774, doi:10.1073/pnas.1103910108 (2011).

275

7 Mahecha, M. D. *et al.* Global Convergence in the Temperature Sensitivity of Respiration at Ecosystem Level. *Science* **329**, 838--840 (2010).

8 Davidson, E. & Janssens, I. Temperature sensitivity of soil carbon decomposition and feedbacks to climate change. *Nature* **440**, 165-173, doi:DOI 10.1038/nature04514 (2006).

9 Jenkinson, D., Adams, D. & Wild, A. Model Estimates Of CO_2 Emissions from soil in response to global

280 Warming. *Nature* **351**, 304--306 (1991).

10 Allison, S. D., Wallenstein, M. D. & Bradford, M. A. Soil-carbon response to warming dependent on microbial physiology. *Nature Geosci* **3**, 336--340 (2010).

11 Wieder, W. R., Bonan, G. B. & Allison, S. D. Global soil carbon projections are improved by modelling microbial processes. *Nature Clim. Change* **3**, 909--912, doi:10.1038/nclimate1951 (2013).

285 12 Tang, J. & Riley, W. J. Weaker soil carbon-climate feedbacks resulting from microbial and abiotic interactions. *Nature Clim. Change* **5**, 56-60, doi:10.1038/nclimate2438 (2015).

13 Bradford, M. A. *et al.* Thermal adaptation of soil microbial respiration to elevated temperature. *Ecology Letters* **11**, 1316--1327, doi:10.1111/j.1461-0248.2008.01251.x (2008).

14 Hugelius, G. *et al.* Estimated stocks of circumpolar permafrost carbon with quantified uncertainty ranges

290 and identified data gaps. *Biogeosciences* **11**, 6573--6593, doi:10.5194/bg-11-6573-2014 (2014).

15 Jones, C. *et al.* Twenty-First-Century Compatible CO_2 Emissions and Airborne Fraction Simulated by CMIP5 Earth System Models under Four Representative Concentration Pathways. *Journal of Climate* **26**, 4398--4413, doi:10.1175/JCLI-D-12-00554.1 (2013).

16 Bradford, M. A. *et al.* Managing uncertainty in soil carbon feedbacks to climate change. *Nature Clim.*

295 *Change* **6**, 751--758 (2016).

17 Todd-Brown, K. E. O. *et al.* Causes of variation in soil carbon simulations from CMIP5 Earth system models and comparison with observations. *Biogeosciences* **10**, 1717--1736, doi:10.5194/bg-10-1717-2013 (2013).

18 He, Y. *et al.* Radiocarbon constraints imply reduced carbon uptake by soils during the 21st century. *Science*

300 **353**, 1419-1424 (2016).

19 Crowther, T. W. *et al.* Quantifying global soil carbon losses in response to warming. *Nature* **540**, 104--108 (2016).

20 Jenny, H. *Factors of soil formation: a system of quantitative pedology.* (Courier Corporation, 1941).

21 Post, W. M., Emanuel, W. R., Zinke, P. J. & Stangenberger, A. G. Soil carbon pools and world life zones.

305 *Nature* **298**, 156--159 (1982).

22 RAICH, J. W. & SCHLESINGER, W. H. The global carbon dioxide flux in soil respiration and its relationship to vegetation and climate. *Tellus B* **44**, 81--99, doi:10.1034/j.1600-0889.1992.t01-1-00001.x (1992).

23 Doetterl, S. *et al.* Soil carbon storage controlled by interactions between geochemistry and climate. *Nature*

310 *Geosci* **8**, 780--783 (2015).

24 Giardina, C. P. & Ryan, M. G. Evidence that decomposition rates of organic carbon in mineral soil do not vary with temperature. *Nature* **404**, 858--861 (2000).

25   LLOYD, J. & TAYLOR, J. ON THE TEMPERATURE-DEPENDENCE OF SOIL RESPIRATION. *Functional Ecology* **8**, 315-323 (1994).

315   26   Harden, J. W. *et al.* Field Information Links Permafrost Carbon to Physical Vulnerabilities of Thawing. *Geophys. Res. Lett.* **39**, doi:10.1029/2012GL051958 (2012).

27   Koven, C. D. *et al.* The effect of vertically-resolved soil biogeochemistry and alternate soil C and N models on C dynamics of CLM4. *Biogeosciences* **10**, 7109-7131, doi:10.5194/bg-10-7109-2013 (2013).

28   Koven, C. D., Lawrence, D. M. & Riley, W. J. Permafrost carbon−climate feedback is sensitive to deep soil

320   carbon decomposability but not deep soil nitrogen dynamics. *Proceedings of the National Academy of Sciences* **112**, 3752--3757 (2015).

29   Wang, Y. P. *et al.* Responses of two nonlinear microbial models to warming and increased carbon input. *Biogeosciences* **13**, 887--902, doi:10.5194/bg-13-887-2016 (2016).

30   Sistla, S. A. *et al.* Long-term warming restructures Arctic tundra without changing net soil carbon storage.

325   *Nature* **497**, 615--618 (2013).

Methods

A central goal of this paper is to use observed spatial gradients in soil carbon turnover, in particular the relationship between apparent turnover and temperature, to develop a benchmark for dynamical models that are used to make projections of soil carbon storage in response to climate change. We recognize that benchmarks derived from spatial gradients are insufficient to constrain transient responses, which is also why the direct use of spatial gradients to extrapolate forward in time (so-called space-for-time substitutions) is not possible. However, transient models must also make predictions about steady-state differences in soil carbon turnover across spatial climate gradients, which reflect a long-term climatological temperature sensitivity. Because such gradients are observable, we seek to use this information as a test of the dynamical models. We contend that this inverse "time-for-space" substitution can serve as a global, observationally-derived benchmark to ask where and whether the underlying processes represented in ESMs are consistent with the observations. We note that the transient dynamics predicted by a given model may differ from that model's steady-state spatial-gradient predictions, due to slow processes such as mineral associations that are important in governing spatial gradients, and whose transient effects may be highly timescale-dependent. We also note that the benchmarking approach here is fundamentally a consistency test, which is a necessary but insufficient constraint on model dynamics, that does not imply that any given model formulation provides a unique solution. We thus advocate that future experimental work also focus on understanding the transient soil carbon dynamics across the world's climate regimes, and in particular focus on monitoring both the productivity and turnover responses to climate change.

Soil carbon stocks are estimated by combining the Harmonized World Soilds Database (HWSD)[1] and Northern Circumpolar Soil Carbon Database (NCSCD)[2] soil carbon maps, using NCSCD where overlap occurs, and estimating productivity via the MODIS net primary productivity (NPP) product[3] (fig. 1a & 1b). Mean annual air temperatures (MAAT) are estimated from the CRU dataset[4]. Both NPP and soil carbon show relationships with temperature, however the log(NPP)-temperature relationship shows a more continuous slope (fig. 1a) than the log(soil carbon)-temperature relationship (fig. 1b), which shows a clear difference between temperate-tropical and a cold-climate soils. Inferred τ is plotted on a log scale because we expect it to have a roughly exponential relationship with temperature, following that of

respiration, and spans a range of about 2 orders of magnitude (fig. 1c & 1d). The full global dataset (Fig. 1c and S1a) shows a main set of points that span a curve of minimum turnover times for a given temperature, with a tail of points extending above this main population. Water also exerts a strong control on soil carbon turnover, with reduced decomposition in soils that are either dry or saturated. Since our main goal here is to focus on temperature controls to decomposition, we seek to separate and mask out those soils that are most strongly affected by having either too much or too little water.

6   To isolate soils whose decomposition is limited by saturation, we use the thematic

7 classification in the NCSCD and HWSD databases to exclude those gridcells that have an areal

8 coverage of more than 50% peat soils, defined as the Histosol soil order or the Histel suborder of

9 Gelisols (permafrost soils) (fig. S1b). To identify soils whose decomposition is limited by

10 aridity, we derive the rainfall regime in each gridcell using the GPCC dataset [5] (fig. 1c). We

11 note that, while long turnover times are associated with both cold climates or very dry climates,

12 only the former actually have large organic carbon stocks (fig. S1c). Furthermore, in cold

13 climates, soils may receive relatively little rainfall but still have abundant moisture because

14 evaporative demand in these climates is low. Thus, we mask out only those soils where demand

15 exceeds supply and soils are dry. We calculate the demand as a potential evapotranspiration

16 (PET) using the MODIS PET product[6], and show the inferred τ-temperature relationship as

17 controlled by precipitation minus PET (fig. S1d). This supports the expectation that long-

18 turnover low latitude soils are predominantly found in dry climates with a strong moisture

19 deficit. Finally, we exclude all points where this moisture deficit falls below a threshold level (-

20 1000 mm y^{-1}), to arrive at the filtered dataset that we use to define the regression curve in fig. 1d.

21   Once the points where τ is not primarily a function of temperature are removed, the

22 relationship between τ and temperature becomes clear. The relationship in $\log(\tau)$ versus

23 temperature is negative, with positive curvature. Although a linear regression shows high

24 significance (r^2=0.62), it also leaves a residual error with systematic structure. We thus reject a

25 linear model relating $\log(\tau)$ to temperature, and find that a quadratic model (fig. 1d, and table S1)

26 fits the relationship well, with r^2=0.68 and little systematic residual bias. Thus, the relationship

27 between inferred τ and temperature is stronger than the hypothesized exponential in temperature

28 over the range of climate conditions.

29   We calculate the curve in figure 2 based on the derivative of the central relationship in

30   figure 1b. Q_{10} is an exponential notation that is traditionally defined relative to the instantaneous

31   decomposition parameter k as:

$$k(T) = k(T_{ref})Q_{10}^{\left(\frac{T-T_{ref}}{10}\right)}$$

32

33   The Q_{10} parameter can therefore be calculated as:

34

$$Q_{10} = \left(\frac{k(T)}{k_{ref}}\right)^{\frac{10}{(T-T_{ref})}}$$

35

36   Since, by definition:

$$k = \frac{1}{\tau}$$

37

38   we can redefine Q_{10} in terms of τ:

$$Q_{10} = \left(\frac{\tau_{ref}}{\tau(T)}\right)^{\frac{10}{(T-T_{ref})}}$$

39

40   and calculate the Q_{10} at any point along the curve as the derivative of $\log(\tau)$ with respect to

41   temperature via:

$$Q_{10} = 10^{\left(-10\frac{d \log (\tau)}{d T}\right)}$$

42

43   By choosing a polynomial regression in figure 1 of the form:

44

$$\log(\tau) = aT^2 + bT + c$$

45

46   these equations combine as:

$$Q_{10} = 10^{-10(2aT+b)}$$

47

48   which is shown in figure 2.

49

50   We identify in figure 3 a framework to understand the implications of alternate ways of

51   representing the temperature sensitivity of soil carbon decomposition on resulting spatial

52   patterns. For results shown in figure 3, we diagnose daily decomposition rate values (*k*) as a

53   function of daily soil temperatures, which are taken from a land model, CLM4.5, driven by bias-

54   corrected reanalysis meteorological data (CRU-NCEP, available at

55   http://dods.ipsl.jussieu.fr/igcmg/IGCM/BC/OOL/OL/CRU-NCEP/). We then calculate the

56   equilibrium τ as the reciprocal of time-averaged *k* values, and plot log(τ) as a function of the

57   driving MAAT. In each case, the *k*, and therefore τ, values are relative to an arbitrary offset to

58   align with the central estimate from figure 1d at 15 ˚C.

59   In the simplest case, we use a fixed Q_{10} value (Q_{10}=1.5) across all temperatures, and we

60   diagnose *k* and τ using near-surface (10 cm depth) soil temperatures (fig. 3a). Log(τ) values show

61   the expected linear relationship against air temperature with only two emergent features. First, all

62   τ values fall slightly below the line relating MAAT to the log(τ) as diagnosed from that MAAT.

63   This offset is a result of the seasonal cycles in soil temperatures, which give a time-average τ that

64   is less than τ calculated from time-averaged temperatures, because the shape of the relationship

65   *k*=f(T) has a positive curvature. Secondly there is a step offset at the transition from temperate to

66   cold climates attributable to the insulating effect of snow, which, where seasonally present,

67   elevates mean soil temperatures above mean air temperatures [7].

68   As a next step in complexity, we consider a temperature-dependent Arrhenius-like

69   relationship[8]:

$$k = k_{ref}e^{308.56\left(\frac{1}{56.02}-\frac{1}{T-227.13}\right)}$$

70   as a potentially more realistic model than a fixed Q_{10} model across all temperatures (Fig. 3b).

71   Such an approach is a better match to the climatological temperature sensitivity in the cold-

72   climate regime, but fares worse as compared to the observation-based relationship in the warm-

73   climate regime. We note as well that, particularly in cold climates, the modeled annual-mean τ

74   values fall well below the blue line that represents the τ evaluated from the annual mean

75   temperature. This suggests that such chemical-kinetic factors, on their own, are not responsible

76   for the observed climatological cold-climate sensitivity.

       A third step in complexity is to explicitly consider the role of soil freezing. Freezing is a

powerful inhibitor of decomposition, and thus we can define the simplest freezing model as one

77   where Q_{10} is fixed ($Q_{10} = 1.5$, as in fig 3a) for thawed soils and ceases in frozen soils ($k = 0$ when

78     $T_{soil} < 0˚C$). This is a simplifying assumption; in natural ecosystems, limited decomposition

79   occurs even in frozen soils, but the $\log(\tau)$ versus MAAT resulting from the no-frozen-respiration

80   case (fig. 3c) is a useful approximation. The result is a slight positive curvature to the

81   relationship that compensates for the snow insulation offset. But the model still fails to match the

82   large increase in temperature sensitivity seen in the observations.

83   The fourth piece of complexity in figure 3 is to consider the vertical variation in soil

84   temperatures in addition to the seasonal variation. To do this, we diagnose k values at each model

85   soil level (9 levels) across the 0-1m soil depth interval, and then calculate τ as the reciprocal of

86   the mean k value averaged both in time and over the depth interval (fig. 3d). This gives a curve

87   of $\log(\tau)$ versus MAAT that approximates the observed one. We note that this behavior arises

88   from the step-function-like behavior in $k=f(T)$ due to freezing, which gives particularly high

89   sensitivity to small temperature changes around the freezing point.

90   Comparing the quadratic regression coefficients for the simplified models shown in figure 3

91   (table S1 and figure S4), the value of the quadratic parameter increases with each level of

92   complexity. While each of the simplified models shown in figure 3 underestimates the curvature

93   as seen in the observations, only the fourth model begins to approach the observation-derived

94   curvature in the temperature sensitivity. This emphasizes the importance of representing how

95   freeze/thaw state scales both temporally and vertically in governing soil carbon decomposition.

96   For the models shown in figure 4, inferred τ is calculated as the ratio of carbon stocks to

97   NPP for each model over the recent historical period, in order to match the observation-based

98   results discussed above, and individual gridcells are colored by a given ESM's precipitation as in

99   figure 1c, (fig. 4a-f). The CMIP5 models used here are listed in table S2. For CMIP5 models

100   (fig. 4a-4f) and MIMICS (fig. 4i), we diagnose τ using total soil carbon stocks, since the models

101   do not provide depth-resolved soil carbon output. For CLM4.5 (fig. 4g-4h), we use stocks to 1m

102   as the carbon stocks in the inferred τ calculation. We note that the lower boundary for soil

103   carbon both in the CMIP5 protocol and in any soil model that does not explicitly resolve depth

104   is not clearly defined, and that there may be errors in correspondence between our comparison of

105   model output and 0-1m integrated soil carbon stocks which could be reduced by models

106   explicitly defining the depth integral over which their stocks correspond; nonetheless we believe

107   this represents the best benchmark on the models.

108   To create a metric of how well each model captures the pattern in the observed relationship

109   (Table S1), we use a binned RMSE scoring approach following [9]. We first filter all points in each

110   model using the same P-PET threshold using model-predicted P and MODIS PET as in the

111   observations (masked data shown fig. S5). Next, we defined bins of 1˚C MAAT over the

112   interval of -15.5C to 28.5C, and for each model, took the mean value of $\log(\tau)$ within each bin to

113   calculate an error score, e, as the RMSE for each bin i of the model prediction p_i relative to the

114   observational estimate o_i of the central estimate from fig. 1 evaluated at the bin center:

$$e = \sqrt{p_i^2 - o_i^2}$$

115   In addition to the RMSE score, we also report in table S1 quadratic fit parameters between

116   MAAT and $\log(\tau)$ for each of the models (regression curves shown in fig. S5), as well as the data

117   shown in figure 1D. For the regression, we mask arid areas using the same P minus PET criteria.

118   In all cases, the quadratic coefficient a derived from the regression is less than that from the

119   observations, and in some cases has the wrong sign; the three models that most closely approach

120   the magnitude of the quadratic term are GFDL-ESM2G, MIMICS and CLM4.5. We also report

121   the residual variance in $\log(\tau)$ after subtracting the regression relationship, for the models and

122   data. Each of these metrics provides different benchmarking constraints on the dynamical

123   models; we leave them as separate constraints rather than merging into a single benchmark here.

Each of the models shown in figure 4 has unique characteristics, and some better

approximate the observed curve than others. Four models (CCSM4[10], MPI-ESM[11], HadGEM2[1],

and IPSL-CM5A-LR[12]) show temperature responses that approximate the simple Q_{10}

relationship. The GFDL-ESM2G[13] model captures the range in turnover in cold-climates well.

This model calculates k values based on a function of the mean temperature over a root-profile

weighted depth interval (E. Shevliakova, personal communication), so includes more

information about deeper soil climate than models that diagnose k values based only on near-

surface information; however we also note that much of the high cold-climate sensitivity in this

models appears to be due to a large offset that occurs at around 0˚C, which may also arise from

the anomalously cold high-latitude soil temperatures in that model[14,15]. MIROC-ESM[16] also

captures some aspects of the cold-climate sensitivity, particularly over the range of temperatures

5˚C to -5˚C, which is consistent with its use of the Lloyd-Taylor equation for its temperature

sensitivity[16]; however, we note that its temperature sensitivity reverses direction in the -5˚C to -

124 10˚C range, and decreases below that. With the exception of MPI-ESM and MIMICS, all models

125 appear to underestimate the sensitivity of decomposition to dry conditions, as indicated by the

126 lack of long-turnover soils in arid conditions that is seen in fig. 1c. CLM4.5 tends to

127 underestimate turnover in the region near MAAT ~-5˚C, which indicates an underestimate on the

128 limitation of decomposition in warm permafrost conditions in that model.

129   All data and analysis scripts required to generate figures in this manuscript are available

130 online at: http://portal.nersc.gov/archive/home/c/cdkoven/www/soil_tau_temp

131

132

133

134

References (Methods)

1   FAO, IIASA, ISRIC, ISSCAS & JRC. Harmonized World Soil Database (version 1.2). (FAO and IIASA, Rome, Italy and Laxenburg, Austria, 2012).

2   Hugelius, G. *et al.* The Northern Circumpolar Soil Carbon Database: spatially distributed datasets of soil coverage and soil carbon storage in the northern permafrost regions. *Earth Syst. Sci. Data* **5**, 3--13, doi:10.5194/essd-5-3-2013 (2013).

3   Zhao, M., Heinsch, F., Nemani, R. & Running, S. Improvements of the MODIS terrestrial gross and net primary production global data set. *Remote Sensing of Environment* **95**, 164--176, doi:DOI 10.1016/j.rse.2004.12.011 (2005).

4   Jones, P. D. H., I. Climatic Research Unit (CRU) time-series datasets of variations in climate with variations in other phenomena. (University of East Anglia Climatic Research Unit, British Atmospheric Data Centre, date of citation, 2008).

5   Schneider, U. *et al. FD_M_V6_050*, doi:10.5676/DWD_GPCC/FD_M_V6_050 (2011).

6   Mu, Q., Zhao, M. & Running, S. W. Improvements to a MODIS global terrestrial evapotranspiration algorithm. *Remote Sensing of Environment* **115**, 1781--1800, doi:http://dx.doi.org/10.1016/j.rse.2011.02.019 (2011).

7   Slater, A. *et al.* The representation of snow in land surface schemes: Results from PILPS 2(d). *Journal of Hydrometeorology* **2**, 7-25 (2001).

8   LLOYD, J. & TAYLOR, J. ON THE TEMPERATURE-DEPENDENCE OF SOIL RESPIRATION. *Functional Ecology* **8**, 315-323 (1994).

9   Slater, A. G., Lawrence, D. M. & Koven, C. D. Process-level model evaluation: A Snow and Heat Transfer Metric. *The Cryosphere Discuss.* **2016**, 1-16, doi:10.5194/tc-2016-258 (2016).

10   Oleson, K. W. *et al.* Technical Description of version 4.0 of the Community Land Model (CLM). (NATIONAL CENTER FOR ATMOSPHERIC RESEARCH, P. O. Box 3000 BOULDER, COLORADO 80307-3000, 2010).

11   Raddatz, T. J. *et al.* Will the tropical land biosphere dominate the climate-carbon cycle feedback during the twenty-first century? *Climate Dynamics* **29**, 565-574, doi:DOI 10.1007/s00382-007-0247-8 (2007).

12   Krinner, G. *et al.* A dynamic global vegetation model for studies of the coupled atmosphere-biosphere system. *Global Biogeochem. Cy.* **19**, GB1015, doi:10.1029/2003GB002199 (2005).

13   Milly, P. C. D. *et al.* An Enhanced Model of Land Water and Energy for Global Hydrologic and Earth-System Studies. *Journal of Hydrometeorology* **15**, 1739--1761, doi:10.1175/JHM-D-13-0162.1 (2014).

14   Slater, A. G. & Lawrence, D. M. Diagnosing Present and Future Permafrost from Climate Models. *Journal of Climate* **26**, 5608--5623, doi:10.1175/JCLI-D-12-00341.1 (2013).

15   Koven, C. D., Riley, W. J. & Stern, A. Analysis of permafrost thermal dynamics and response to climate change in the CMIP5 Earth System Models. *Journal of Climate*, doi:10.1175/JCLI-D-12-00228.1 (2012).

16   Sato, H., Itoh, A. & Kohyama, T. SEIB--DGVM: A new Dynamic Global Vegetation Model using a spatially explicit individual-based approach. *Ecological Modelling* **200**, 279--307, doi:http://dx.doi.org/10.1016/j.ecolmodel.2006.09.006 (2007).